Topographic Amplification of Earthquake Ground Motion on Hills of Bell-Shaped Geometry

Kavan Modha[1[0000-0001-9492-9993]], Dhiraj Raj[1[0000-0002-5296-8588]] and Yogendra Singh[1[0000-0001-6722-8956]]

[1] Indian Institute of Technology Roorkee, Roorkee 247667, India
kavanmodha@gmail.com
Dhirajraj.iitr@gmail.com
Yogendra.eq@gmail.com

Abstract. Alteration in ground motion characteristics due to topography can trigger earthquake induced localized damage and other earthquake related devastation. Existing literature cites many incidents in which topographic amplification has been noticed during the same seismic event. However, it is often difficult to separate the effects of geometry and near-surface geology in absence of refined topographic amplification models. Based on hill geometry, a few standards/codes (Eurocode 8, NTC-08 and AFPS) suggest the amplification factors or aggravation factors to address this issue. However, topographic amplification of hills subjected to recorded ground motion are mostly lacking in literature.

This paper presents a parametric study of 2D symmetrical bell shaped hills having different shape ratios (ratio of height to half of the base width of the hill) using finite element code ABAQUS. Wave propagation problem is simulated using 2D linear plane strain elements. Numerical models are subjected to the recorded earthquake ground motion suite (22 far-field record) from FEMA P695 along viscous boundaries at base. Parasitic boundaries are used at vertical sides to ensure shear failure mode. The largest size of the element is limited to 1/15th times the desired wavelength (10 Hz) of selected ground motion suite. Topographic amplification (ratio of PGA obtained at the peak of the hill to that of the free field) values are quantified at different spatial points along the hill profile to study the variation in amplification of PGA values. It is observed that topography is mostly amplifying the PGA values at the peak of the hill and de-amplifying the PGA values at the foot of the hill.

Keywords: Topographic amplification; Shape ratio; Recorded ground motion; Finite element method

1 Introduction

Generally, seismic waves are generated by energy release from tectonic plate at shallow depth to several kilometers beneath the ground surface. These waves travel through various heterogeneous materials with different travel velocities. Seismic waves travel faster in denser medium than rarer medium. Naturally, denser medium is overlain by rarer medium and waves propagating from denser (at large depth) to rarer

medium becomes almost vertically upward. When seismic wave travel through various heterogeneous materials, ground motion characteristics (amplitude, frequency content and duration) are altered significantly. In addition, surface topography also alters the ground motion characteristics significant and cause damage in hilly regions during the recent earthquakes [1].

In the last six decades, many studies exhibited that topographic features like cliffs, canyons, ridges, hills, slopes alter the ground motion significantly. Based on the considered topography, ground motion can amplify or de-amplify. The former has been observed often near hilltops and close to the ridges, which contributed to the higher damages during seismic events. Several researchers have observed topographic amplification by comparing the ground motion recorded on elevated and flat grounds during the same seismic events [2-8]. However, it is often difficult to separate the contribution of topographic features and near surface geology in case of the recorded ground motion.

Several experimental studies [9-13] and numerical studies using different methods like Finite Elements Method (FEM) [7,14-16], Aki-Larner Technique [17,18], Boundary Integral method [6], Finite Difference Method [3,19-21], Generalized Consistent Transmitting Boundary (GCTB) given by Deng [22,23] etc. have been conducted in the past. Most of the numerical studies have been carried out on quantification of topographic amplification using simple harmonic motion [15], Ricker wavelet [22-25,16,26], Gabor wavelet [14] or Chang's equation [19,27] as an input which contains one predominant frequency to avoid large computational efforts. Only a few studies have been performed on quantification of topographic amplification using earthquake ground motions (consisting of multiple frequencies) as input [20,19].

Significant deviations in the topographic amplification factors are responsible for their address in only few building codes across the world [28] and then only in simplified way. Due to complexity, consideration of topographic amplification in design has been recommended by only few of seismic building codes (viz. Italian code [29], Eurocode [30] and French code [31]) in terms of aggravation factors based on hill geometry. However, the amplitudes of maximum aggravation factors are in same range for all the standards. In all standards, topographic amplification factors are solely given as a function of shape ratio (ratio of '*h*' to '*b*', where '*h*' is the height of the hill and '*b*' is the half of the base width of the hill) or slope angle (¯) of the topographic feature neglecting the characteristics of the incident waves, such as frequency [19], wave type [32], orientation [33] or angle of incidence [22].

It is interesting to note that most of the above studies have been performed for single faced slope, but in reality for hill slopes have very complex geometries in 3-dimension. Further, topographic amplification of hill subjected to recorded ground motion are mostly lacking in literature. Recently, topographic amplification observed during L'Aquila earthquake (2009) was significantly mismatching with that given in Italian seismic code [1], highlights the need of an in-depth study on quantification of topographic amplification. To bridge this gap, an extensive numerical study has been performed on a simplified bell shaped hill geometry subjected to recorded ground motion suite using FEM. Based on this study, the results are presented in the form of amplification of PGA over the entire hill profile.

2 Numerical Study

Topographic amplification factor (TAF) is defined either as ratio of the PGA [19,16] or Fourier spectra [3,18,5,15] or response spectra [20] of the ground motion recorded at hill top to the free field. In the present study, TAF has been used in the terms of the PGA ratio.

An extensive parametric study has been conducted to estimate the TAF for the bell shaped hill with four different base widths (2*b*) viz. 500 m, 1000 m, 1500 m and 2000 m and six different shape ratios viz. 0.25, 0.50, 0.75, 1.00, 1.50 and 2.00. Fig. 1 shows schematic diagram of FE model for the idealized hill slope with dimension.

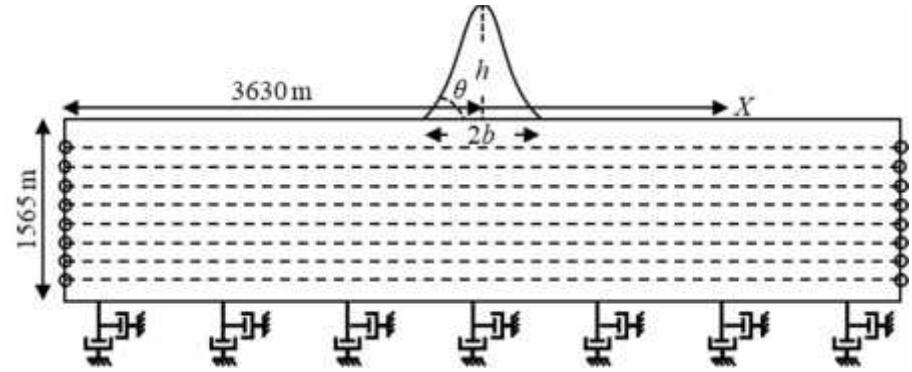

Fig. 1. Schematic diagram of FE model of bell shaped hill with applied boundary conditions

To simulate wave propagation problem (vertically propagating shear waves or SV waves) through homogeneous intact rock properties, Finite Element software Abaqus [34] has been used. To represent stable mild to steep slopes, the material properties of homogeneous intact rock are taken as: shear wave velocity, V_s = 2824 m/s, Poisson's ratio, ν = 0.258, mass density, ρ = 2457 kg/m^3 [26,35-37]. A suite of ground motions consisting of 22 far field recorded acceleration time histories (from FEMA-P695 [38]) has been used as the input motion applied at the base of the developed FE models. These ground motions have been recorded during fourteen different seismic events (occurred between 1971 and 1999) whose moment magnitude, M_w is ranging from 6.5 to 7.6 and PGA is ranging from 0.21g to 0.82g.

3 Modelling and Analysis

In the present study, 2D FE models of considered Bell shaped hill geometry have been developed using Abaqus [34]. An elastic constitutive model based on Hook's law has been used for rock mass modeling. Entire rock mass domain has been discretized using plane strain triangular elements CPE3 (3-node linear) and quadrilateral elements CPE4R (4-node bilinear, reduced integration with hourglass control) available in Abaqus element library. In order to avoid the numerical distortion of frequency

content in simulation of wave propagation problems, Kuhlemeyer and Lysmer [39] suggested the maximum size of the element should be limited to $1/8^{th}$ to $1/12^{th}$ of λ, where λ is the desired wavelength of the propagating seismic wave. Later on, Semblat and Brioist [40] suggested the range of $1/10^{th}$ to $1/20^{th}$ of the wavelength of the propagating waves for large propagating distances. Further, based on preliminary sensitivity study, the largest size of the element has been estimated to $1/15^{th}$ of the smallest wavelength based on the highest frequency of interest available in the earthquake ground motion (considered 10 Hz in the present study). At the base of the FE model, viscous or absorbing boundary [41] has been applied, whereas parasitic boundary [42] has been adopted for the vertical sides of the model. The lateral extent of model has been considered using a sensitivity study so that the effect of boundary conditions on the domain of interest is insignificant.

Frequency dependent Rayleigh damping has been used for rock mass with the critical damping ratio of 0.1%. Rayleigh damping coefficients, α and β, have been obtained from the Eqs. 1 and 2 as:

$$\sim = \frac{2 \times \mu_i \times \mu_j}{\mu_i + \mu_j} \P \tag{1}$$

$$= \frac{2 \times \P}{\mu_i + \mu_j} \tag{2}$$

where, ξ is the critical damping ratio and ω_i and ω_j correspond to the range of rotational frequencies of interest (considered 0.1 Hz and 10 Hz, respectively). For compliant base, input motions have been applied in form of uniformly distributed shear force over un-deformed area of the base of the FE model. For this purpose, the recorded acceleration time history, first, converted to velocity time history by numerical integration and then converted to shear stress history by the Eq. 3 [43].

$$\pm_s(t) = 2 \times \circ \times V_s \times v(t) \tag{3}$$

where, $\sigma_s(t)$ = applied shear stress history, ρ = mass density, $v(t)$ = velocity time history and V_s = shear wave velocity of rock mass.

Linear direct time history analysis based on dynamic implicit method has been conducted to simulate the wave propagation through the rock mass and to estimate the TAF along the entire hill profile.

4 Model Validation

To validate the developed FE model and its effectiveness, a flat ground consisting of same rock mass properties having depth of 1565 m has been modelled in the Abaqus. For vertical sides parasitic boundary has been used and at the base either absorbing (compliant base) or elementary (rigid base) boundary has been applied. Ground motion recorded at Beverly Hills-Mulhol during Northridge earthquake (1994) has been,

first, de-convoluted to the model depth using 1D wave propagation code SHAKE2000. Then, de-convoluted ground motion has been applied to the base of FE model in form of shear stress time history in case of compliant base and in form of acceleration time history in case of rigid base. The acceleration time history has been recorded on the top surface of both models and their comparison has been shown in Fig. 2.

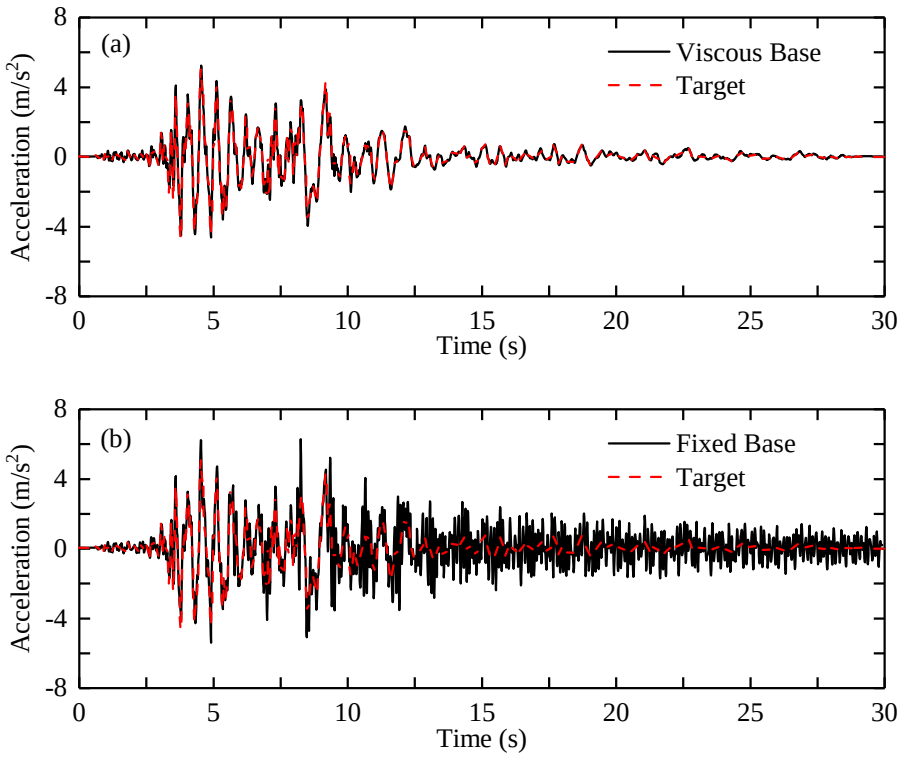

Fig. 2. Comparison of acceleration time history at the top of the model

Fig. 2a shows good agreement between target acceleration time history and time history obtained at the top of the FE model with viscous boundary. In case of fixed base model, significant miss match has been observed owing to generation of very high frequency spurious waves reflected from the fixed boundary (Fig. 2b). However, their response spectra match well for the frequency range of interest (Fig. 3).

In addition, when the synthetic bell shaped hill has been modelled above the flat terrain, spurious periodic waves result in additional amplification in case of fixed base model. However, in case of same compliant base synthetic bell shaped hill model, spurious periodic waves get efficiently absorbed at the viscous boundary and provide more reliable estimation of TAF. This observation is similar to the study of Mejia and Dawson [21] and hence compliant base FE model has been considered in the further study.

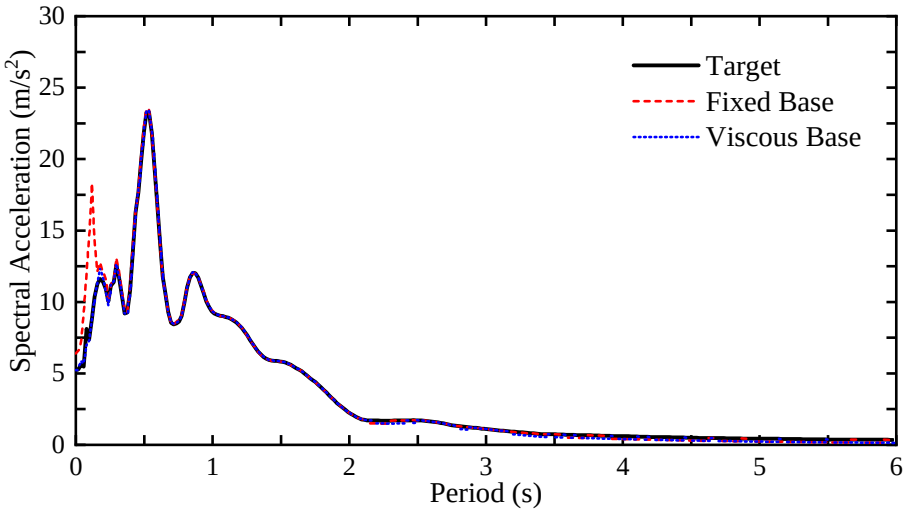

Fig. 3. Comparison of response spectra at the top of the flat model for different boundary condition

5 Results and Discussion

As mentioned earlier, the prime objective of the present study is to estimate the TAF for various bell shaped hill geometries. TAF has been obtained for each case in terms of ratio of PGA observed at any location on the hill surface to the PGA observed on free field. For each geometrical configuration, 22 de-convoluted ground motions have been applied at the compliant base and their mean amplification values have been reported at various locations along the entire hill surface. Figures 5-8 show the variation in TAF along the hill with different shape ratio (SR = 0.25, 0.50, 0.75, 1.00, 1.50 and 2.00) and b = 500, 1000, 1500 and 2000 m, respectively.

From Figures 5-8, it can be observed that TAF increases with increase in slope inclination, θ. The critical incident angle, θ_{cr}, for vertically propagating shear waves depends on the Poisson's ratio of the medium through which the wave travels (Assimaki et al. 2005). In the present study, for ν = 0.258, θ_{cr} has been obtained from Eq, 4 as:

$$-_{cr} = \sin^{-1}\left(\sqrt{\frac{1-2\neg}{2(1-\neg)}}\right) = 34.83° \tag{4}$$

For $\theta > \theta_{cr}$, the more amplification has been observed at the hill top due to incident energy transformation travel along the slope and interference with direct SV waves that arrive behind the crest. Whereas, for $\theta < \theta_{cr}$, only marginal amplification has been observed.

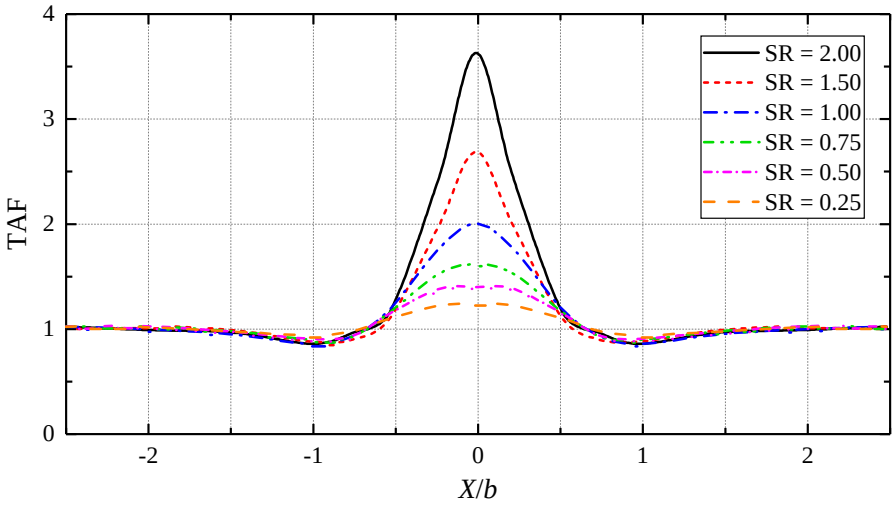

Fig. 4. Variation of amplification along the profile of the hill for different shape ratios and 2b = 500 m

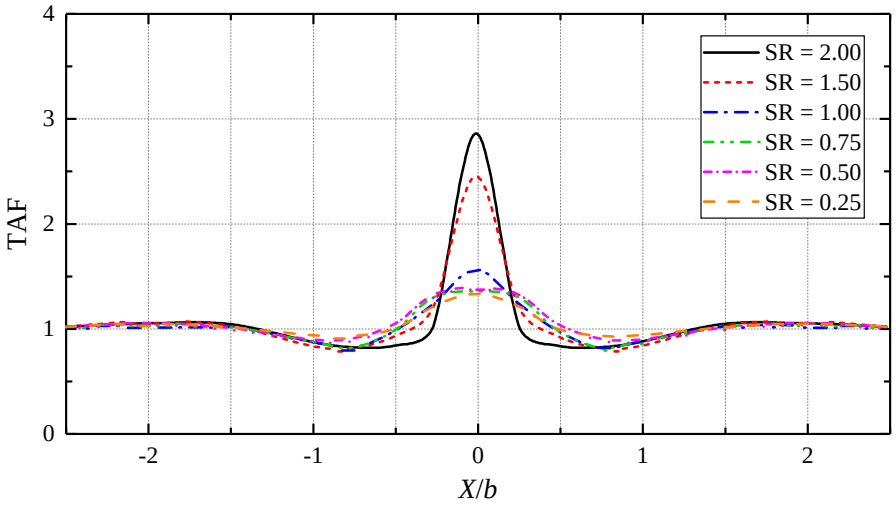

Fig. 5. Variation of amplification along the profile of the hill for different shape ratios and 2b = 1000 m

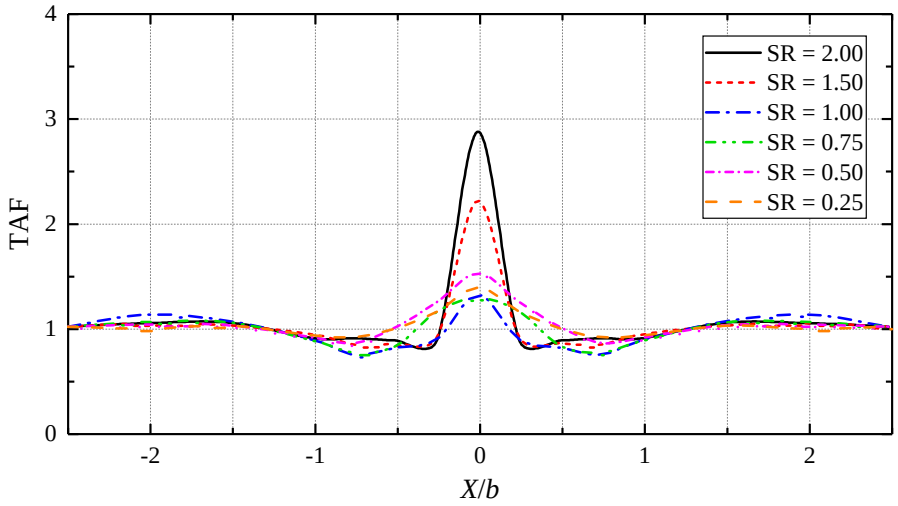

Fig. 6. Variation of amplification along the profile of the hill for different shape ratios and 2b = 1500 m

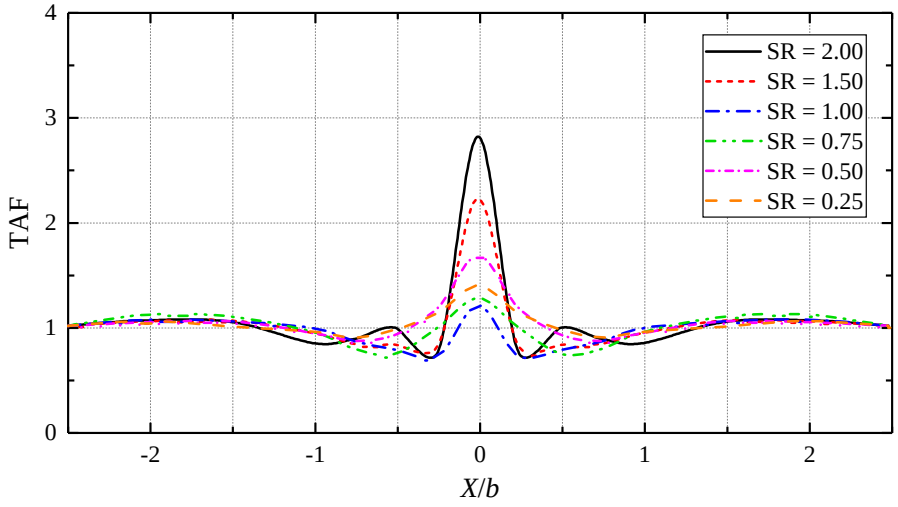

Fig. 7. Variation of amplification along the profile of the hill for different shape ratios and 2b = 2000 m

It is interesting to note that, the hill base width has slight effect on TAF for the same shape ratio. The free field condition (when TAF becomes asymptotic to 1) has been observed at the distance approximately equal to 'b' from the toe of the hill. The maximum TAF along the hill profile has been observed at the peak of the hill and significant de-amplification has been observed near the toe of the hill due to scattering of waves.

6 Conclusion

An extensive numerical study has been performed on a simplified bell shaped hill geometry of homogeneous material subjected to recorded ground motion suite using FEM. Based on the study, the results are presented in the form of amplification of PGA across the hill profile. Highest amplification of incident waves has been observed at the pinnacle because of trapping of the energy and de-amplification has been observed at the toe of the hill due to the scattering of the waves. Amplification tends to increase with the increasing slope inclination whereas almost equal values of amplification have been observed for hills having different base widths but the same inclination. The results obtained from this study are valid only for bell shaped hill geometry with homogeneous rock mass. Therefore, more rigorous study is required to estimate of the TAF for hills consisting of different materials and shapes.

7 Acknowledgement

Assistance ship provided by consultancy project no. EQD/6040/2018-19 to first and research project no. IMP1298#EQD to second author is gratefully acknowledged. Further, authors want to thank excellent computation facilities provided by the Department of Earthquake Engineering, Indian Institute of Technology Roorkee.

References

1. Gallipoli, M.R., Bianca, M., Mucciarelli, M., Parolai, S., Picozzi, M.: Topographic versus stratigraphic amplification: mismatch between code provisions and observations during the L'Aquila (Italy, 2009) sequence. Bulletin of Earthquake Engineering 11(5), 1325-1336 (2013). doi:10.1007/s10518-013-9446-3
2. Trifunac, M.D., Hudson, D.E.: Analysis of the Pacoima dam accelerogram-San Fernando, California, earthquake of 1971. Bulletin of the Seismological Society of America 61(5), 1393-1411 (1971).
3. Boore, D.M.: A note on the effect of simple topography on seismic SH waves*. Bulletin of the Seismological Society of America 62(1), 275-284 (1972).
4. Çelebi, M.: Topographical and geological amplifications determined from strong-motion and aftershock records of the 3 March 1985 Chile earthquake. Bulletin of the Seismological Society of America 77(4), 1147-1167 (1987).
5. Hartzell, S.H., Carver, D.L., King, K.W.: Initial investigation of site and topographic effects at Robinwood Ridge, California. Bulletin of the Seismological Society of America 84(5), 1336-1349 (1994).
6. Bouchon, M., Barker, J.S.: Seismic response of a hill: The example of Tarzana, California. Bulletin of the Seismological Society of America 86(1A), 66-72 (1996).
7. Gazetas, G., Kallou, P.V., Psarropoulos, P.N.: Topography and Soil Effects in the MS 5.9 Parnitha (Athens) Earthquake: The Case of Adámes. Natural Hazards 27(1), 133-169 (2002). doi:10.1023/A:1019937106428

8. Assimaki, D., Gazetas, G.: Soil and Topographic Amplification on Canyon Banks and the 1999 Athens Earthquake. Journal of Earthquake Engineering 08(01), 1-43 (2004). doi:10.1142/S1363246904001250
9. Nogoshi, M.: On the amplitude characteristics of microtremor, Part II. Journal of the seismological society of Japan 24, 26-40 (1971).
10. Nakamura, Y.: A method for dynamic characteristics estimation of subsurface using microtremor on the ground surface. Railway Technical Research Institute, Quarterly Reports 30(1) (1989).
11. Pagliaroli, A., Pitilakis, K., Chávez-García, F., Raptakis, D., Apostolidis, P., Ktenidou, O.-J., Manakou, M., Lanzo, G.: Experimental study of topographic effects using explosions and microtremors recordings. In: Fourth International Conference on Earthquake Geotechnical Engineering, Thessaloniki, Greece 2007
12. Jafarzadeh, F., Shahrabi, M.M., Farahi Jahromi, H.: On the role of topographic amplification in seismic slope instabilities. Journal of Rock Mechanics and Geotechnical Engineering 7(2), 163-170 (2015). doi:10.1016/J.JRMGE.2015.02.009
13. Borcherdt, R.D.: Effects of local geology on ground motion near San Francisco Bay. Bulletin of the Seismological Society of America 60(1), 29-61 (1970).
14. Tripe, R., Kontoe, S.: A numerical investigation into the interaction between topographic and soil layer amplification of earthquake motion. In: 5th International Conference on Earthquake Geotechnical Engineering, Santiago, Chile 2011
15. Kaynia, A.M.: Amplification of Seismic Waves by Hills of Different Materials. In., vol. 20120230-01-TN. (2014)
16. Rizzitano, S., Cascone, E., Biondi, G.: Coupling of topographic and stratigraphic effects on seismic response of slopes through 2D linear and equivalent linear analyses. Soil Dynamics and Earthquake Engineering 67, 66-84 (2014). doi:10.1016/J.SOILDYN.2014.09.003
17. Bard, P.-Y.: Diffracted waves and displacement field over two-dimensional elevated topographies. Geophysical Journal of the Royal Astronomical Society 71(3), 731-760 (1982). doi:10.1111/j.1365-246X.1982.tb02795.x
18. Geli, L., Bard, P.-Y., Jullien, B.: The effect of topography on earthquake ground motion: A review and new results. Bulletin of the Seismological Society of America 78(1), 42-63 (1988).
19. Bouckovalas, G.D., Papadimitriou, A.G.: Numerical evaluation of slope topography effects on seismic ground motion. Soil Dynamics and Earthquake Engineering 25(7-10), 547-558 (2005). doi:10.1016/J.SOILDYN.2004.11.008
20. Fotopoulou, S.D., Pitilakis, K.D.: Vulnerability assessment of reinforced concrete buildings at precarious slopes subjected to combined ground shaking and earthquake induced landslide. Soil Dynamics and Earthquake Engineering 93, 84-98 (2017). doi:10.1016/J.SOILDYN.2016.12.007
21. Mejia, L., Dawson, E.: Earthquake Deconvolution for FLAC. In: 4th International FLAC Symposium on Numerical Modeling in Geomechanics, Madrid, Spain 2006
22. Ashford, S.A., Sitar, N.: Analysis of topographic amplification of inclined shear waves in a steep coastal bluff. Bulletin of the Seismological Society of America 87(3), 692-700 (1997).
23. Ashford, S.A., Sitar, N., Lysmer, J., Deng, N.: Topographic effects on the seismic response of steep slopes. Bulletin of the Seismological Society of America 87(3), 701-709 (1997).

24. Narayan, J.P.: Study of Basin-edge Effects on the Ground Motion Characteristics Using 2.5-D Modelling. pure and applied geophysics 162(2), 273-289 (2005). doi:10.1007/s00024-004-2600-8
25. Razmkhah, A., Kamalian, M., Sadroldini, S.M.A.: Application of boundary element method to study the seismic response of triangular hills. In: Proceedings of 14th World Conference on Earthquake Engineering, Beijing, China 2008, vol. August
26. Narsimha, D.S.: Topographic amplification and seismic risk assessment in hills. Ph.D. Thesis, Indian Institute of Technology Roorkee (2015)
27. Tripe, R., Kontoe, S., Wong, T.K.C.: Slope topography effects on ground motion in the presence of deep soil layers. Soil Dynamics and Earthquake Engineering 50, 72-84 (2013). doi:10.1016/J.SOILDYN.2013.02.011
28. Molina, S., Lang, D.H., Singh, Y., Meslem, A.: A period-dependent topographic amplification model for earthquake loss estimation. Bulletin of Earthquake Engineering, 1-17 (2019).
29. NTC2018: Norme Tecniche per le Costruzioni. In: Gazzetta Ufficiale. Il Ministro Delle Infrastrutture, Decreto 17 Gennaio, (2018)
30. CEN: EN 1998-5, Eurocode 8: Design of structures for earthquake resistance - Part 5: Foundations, retaining structures and geotechnical aspects. In. European Committee for Standardization, Brussels, (2004)
31. Association Française du Génie Parasismique: AFPS 90, Recommendations for the redaction of rules relative to the structures and installations built in regions prone to earthquakes. In. French Association for Earthquake Engineering, (1990)
32. Kamalian, M., Jafari, M.K., Sohrabi-Bidar, A., Razmkhah, A.: Seismic response of 2-D semi-sine shaped hills to vertically propagating incident waves: amplification patterns and engineering applications. Earthquake Spectra 24(2), 405-430 (2008).
33. Pedersen, H., Sanchez-Sesma, F., Campillo, M.: Three-dimensional scattering by two-dimensional topographies. Bulletin of the Seismological Society of America 84(4), 1169-1183 (1994).
34. Abaqus: ABAQUS Documentation, Dassault Systèmes. Providence, RI, USA (2016)
35. Ahmad, S.: Numerical simulation of topographic amplification. M.tech. Dissertation, Indian Institute of Technology Roorkee (2017)
36. Modha, K.G.: Spectral Amplification of Ground Motion Due to Triangular Hill Features. M.tech. Dissertation, Indian Institute of Engineering Roorkee (2018)
37. Modha, K.G., Raj, D., Singh, Y.: Topographic Amplification for Triangular Hill Geometry. In: 16th Symposium on Earthquake Engineering, IIT Roorkee, India 2018
38. Federal Emergency Management Agency: Quantification of Building Seismic Performance Factors. In. FEMA P695, Washington, D.C., (2009)
39. Kuhlemeyer, R.L., Lysmer, J.: Finite element method accuracy for wave propagation problems. Journal of the Soil Mechanics and Foundations Division 99(5), 421-427 (1973).
40. Semblat, J.-F., Brioist, J.-J.: Efficiency of higher order finite elements for the analysis of seismic wave propagation. Journal of Sound and Vibration 231(2), 460-467 (2000). doi:10.1006/jsvi.1999.2636
41. Lysmer, J., Kuhlemeyer, R.: Numerical comparison of high-order absorbing boundary conditions and perfectly matched layers for a dispersive one-dimensional medium. Journal of the Engineering Mechanics Division 95, 859-876 (1969).

42. Sextos, A.G., Manolis, G.D., Athanasiou, A., Ioannidis, N.: Seismically induced uplift effects on nuclear power plants. Part 1: Containment building rocking spectra. Nuclear Engineering and Design 318, 276-287 (2017). doi:10.1016/J.NUCENGDES.2016.12.035
43. Flac2D: FLAC - Fast Langragian Analysis of Continua, Version 6 User's Manual. Itasca Consulting Group, Minneapolis (2005)